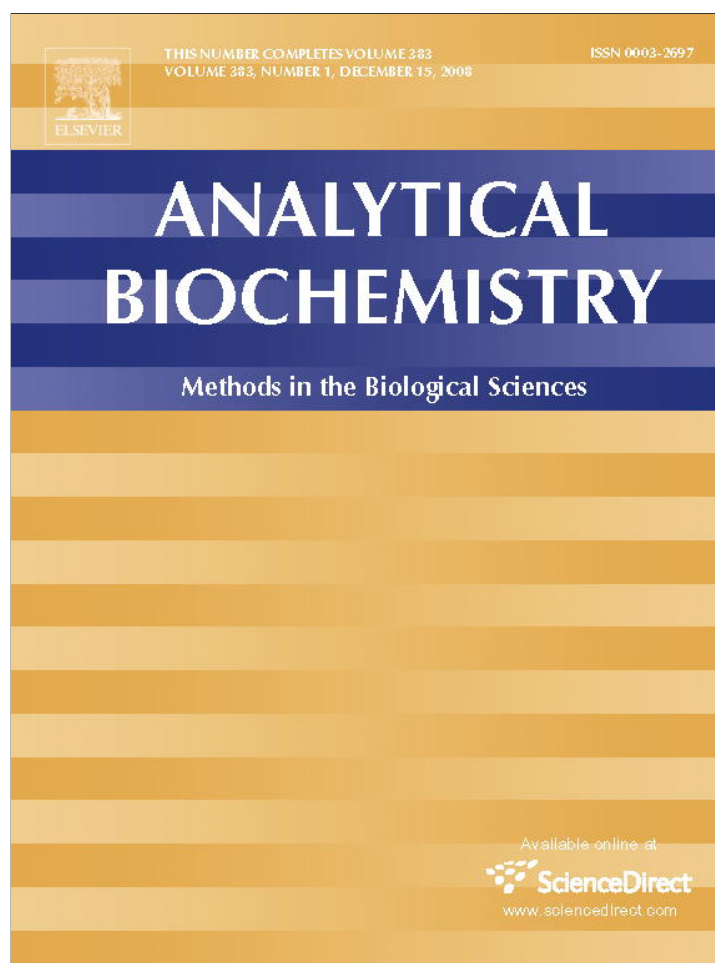


Provided for non-commercial research and education use.
Not for reproduction, distribution or commercial use.



This article appeared in a journal published by Elsevier. The attached copy is furnished to the author for internal non-commercial research and education use, including for instruction at the authors institution and sharing with colleagues.

Other uses, including reproduction and distribution, or selling or licensing copies, or posting to personal, institutional or third party websites are prohibited.

In most cases authors are permitted to post their version of the article (e.g. in Word or Tex form) to their personal website or institutional repository. Authors requiring further information regarding Elsevier's archiving and manuscript policies are encouraged to visit:

<http://www.elsevier.com/copyright>



Contents lists available at ScienceDirect

Analytical Biochemistry

journal homepage: www.elsevier.com/locate/yabio

Methods for assessing DNA hybridization of peptide nucleic acid–titanium dioxide nanoconjugates

Eric M.B. Brown^a, Tatjana Paunesku^{a,b}, AiGuo Wu^a, K. Ted Thurn^a, Benjamin Haley^a, Jimmy Clark^c, Taisa Priester^a, Gayle E. Woloschak^{a,b,d,*}

^a Department of Radiation Oncology, Northwestern University, Feinberg School of Medicine, 303 E. Chicago Avenue, Ward-13-002, Chicago, IL 60611, USA

^b Department of Radiology, Northwestern University, Chicago, IL 60611, USA

^c Department of Biology, North Park University, Chicago, IL 60625, USA

^d Department of Cellular and Molecular Biology, Northwestern University, Chicago, IL 60611, USA

ARTICLE INFO

Article history:

Received 2 June 2008

Available online 26 August 2008

Keywords:

Titanium dioxide

Peptide nucleic acid

Nanoparticle

DNA

Hybridization

ABSTRACT

We describe the synthesis of peptide nucleic acid (PNA)–titanium dioxide (TiO₂) nanoconjugates and several novel methods developed to investigate the DNA hybridization behaviors of these constructs. PNAs are synthetic DNA analogs resistant to degradation by cellular enzymes that hybridize to single-stranded DNA (ssDNA) with higher affinity than DNA oligonucleotides, invade double-stranded DNA (dsDNA), and form different PNA/DNA complexes. Previously, we developed a DNA–TiO₂ nanoconjugate capable of hybridizing to target DNA intracellularly in a sequence-specific manner with the ability to cleave DNA when excited by electromagnetic radiation but susceptible to degradation that may lower its intracellular targeting efficiency and retention time. PNA–TiO₂ nanoconjugates described in the current article hybridize to target ssDNA, oligonucleotide dsDNA, and supercoiled plasmid DNA under physiological-like ionic and temperature conditions, enabling rapid, inexpensive, sequence-specific concentration of nucleic acids *in vitro*. When modified by the addition of imaging agents or peptides, hybridization capabilities of PNA–TiO₂ nanoconjugates are enhanced, providing essential benefits for numerous *in vitro* and *in vivo* applications. The series of experiments shown here could not be done with either TiO₂–DNA nanoconjugates or PNAs alone, and the novel methods developed will benefit studies of numerous other nanoconjugate systems.

© 2008 Elsevier Inc. All rights reserved.

During their lifetime, organisms often acquire unwanted foreign or mutated DNA that may negatively affect their health. Traditional modes of diagnosis are often unable to detect the presence of deleterious DNA; in addition, common treatments for such diseases do not address the underlying cause of disease—changes at the level of the genome—and therefore do not discriminate well between target and healthy cells. This lowers the therapeutic efficacy of such conventional treatments. New types of early detection imaging agents and sequence-specific gene therapies are needed to diagnose and remove unwanted DNA in diseased cells without affecting healthy neighboring cells. Imaging and elimination of unwanted genes and gene products have been major goals of molecular biology over the past few decades, and a sudden proliferation of different RNA interference techniques (reviewed in Refs. [1–3]) attest to that trend. As a result of recent advancements in

nanotechnology, biologists now have access to materials with novel properties that emerge only at the nano scale, enabling innovative imaging and therapeutic approaches [4–6]. In our laboratory, we previously synthesized a DNA–titanium dioxide (TiO₂)¹ nanoconjugate that is suitable for imaging and inflicting inducible, sequence-specific cleavage of unwanted target DNA [7].

TiO₂ nanoparticles smaller than 20 nm covalently attached to single-stranded DNA (ssDNA) via the bidentate enediol ligand dopamine [6,7] are able to bind to complementary DNA sequences. Hybridization between the oligonucleotide of nanoconjugates and complementary DNA inside cells can occur, leading to sequence-specific retention of DNA–TiO₂ nanoconjugates in the nucleus or mitochondria of a cell [7,8]. The TiO₂ nanoparticle has the ability to serve as a multimodal imaging agent because it can be conjugated to imaging molecules such as gadolinium compounds—used

* Corresponding author. Address: Department of Radiation Oncology, Northwestern University, Feinberg School of Medicine, 303 E. Chicago Avenue, Ward-13-002, Chicago, IL 60611, USA. Fax: +1 312 577 0751.

E-mail address: g-woloschak@northwestern.edu (G.E. Woloschak).

¹ Abbreviations used: TiO₂, titanium dioxide; ssDNA, single-stranded DNA; MRI, magnetic resonance imaging; PNA, peptide nucleic acid; dsDNA, double-stranded DNA; EDTA, ethylenediaminetetraacetic acid; pEGF, peptide segment of epidermal growth factor; NLS, nuclear localization signal; ANOVA, analysis of variance; SE, standard errors; Au, gold; aNP, Alizarin Red S-coated TiO₂ nanoparticles.

as contrast agents for magnetic resonance imaging (MRI) [9,10] and optically fluorescent agents that are ortho-substituted enediol ligands [5,6,11].

Although DNA nanoconjugates may serve as possible vehicles to image and remove unwanted DNA, their targeting efficiency and intracellular retention may be lowered by cellular factors such as degradation by intracellular nucleases. To address these potential problems and improve the stability of hybridization with target sequences, we developed a peptide nucleic acid (PNA)-TiO₂ nanoconjugate that may possess advantages over its DNA-TiO₂ counterpart. PNAs are a class of DNA analog that contain the same bases as DNA but, instead of a phosphate diester backbone, possess an achiral polyamide backbone consisting of *N*-(2-aminoethyl) glycine units [12]. These characteristics provide PNAs with benefits over DNAs for many applications. For example, advanced nonionic oligonucleotides such as PNAs possess far better intracellular stability and specificity [13], are more resistant to nuclease and protease attack [14], and have a lower affinity toward DNA-binding proteins [15] than DNA. Due to their neutrally charged backbones and standard bases, PNAs can bind different nucleic acids with high affinity and form various complexes with complementary DNA [16]. PNAs are able to form PNA/RNA [17], PNA/DNA [18], and PNA/PNA duplexes [19] as well as PNA/DNA/PNA triplexes [20]. A PNA/DNA duplex has a higher melting temperature than a DNA/DNA duplex; moreover, modified homopyrimidine bis-PNAs and homopyrimidine bis-PNA-peptide conjugates containing a mixed-base extension of the Watson-Crick polypyrimidine strand have shown the remarkable ability to invade linear double-stranded DNA (dsDNA) [21,22]. Prior to this study, mixed-base PNAs have not been reported to invade dsDNA, but mixed-base PNAs are capable of end invasion of DNA duplexes [23]. In addition, homothymine PNA-antraquinone conjugates have demonstrated the ability to photoinduce cleavage on the displaced DNA strand [21]. Therefore, PNA-TiO₂ nanoconjugates can be expected to bind target nucleic acid sequences with higher avidity than DNA-TiO₂ nanoconjugates while being resistant to nuclease attacks. Presence of the TiO₂ nanoparticle, on the other hand, is expected to provide versatility to the nanoconjugate that far surpasses the benefits of free PNAs. Simultaneous combination of PNA-carrying nanoparticles with a medley of peptides with cell type-specific, cell-penetrating, and subcellular localization capabilities allows fine-tuned targeting that is not possible for free PNAs. The ability of nanoparticles to anchor optically fluorescent molecules or agents with high magnetic resonance contrast is also unique to TiO₂ nanoparticle-conjugated PNAs. Finally, nanoparticle-bound PNAs can also be used as a means for rapid, inexpensive, sequence-specific nucleic acid precipitation *in vitro*.

This study was aimed at characterization of the hybridization abilities of PNA-TiO₂ nanoconjugates with or without the addition of imaging agents and peptides. The presence of the TiO₂ nanoparticle, to which the PNA is firmly tethered, prevents PNA-TiO₂ nanoconjugates from migrating through gels; moreover, absorption of TiO₂ in the wavelength range of nucleic acids [6] prevents spectrophotometry approaches to study PNA-TiO₂/DNA hybridization. Therefore, instead of gel electrophoresis and/or spectrophotometry, we needed to develop alternative approaches to evaluate hybridization properties of these nanoconjugates. It is likely that the approaches developed for this study could benefit investigation of other types of nucleic acid-nanoparticle nanoconjugates. The results of this study demonstrate that PNA-TiO₂ nanoconjugates hybridize to target DNA in a sequence-specific manner, engage in strand exchange and end invasion, and invade supercoiled plasmid DNA containing a mixed-base target under physiological-like ionic and temperature conditions.

Materials and methods

PNAs, DNA oligonucleotides, nanoconjugates, and plasmids

All nucleic acid sequences used within this study are depicted in Table 1. PNA containing a sequence of a segment of ribosomal 18S rDNA gene was synthesized with a dopamine conjugated via succinic acid to the N-terminal end (Biosynthesis). PNA-TiO₂ nanoconjugates were synthesized by covalently linking 3-nm TiO₂ nanoparticles to the PNA in a 1:1 molar ratio as described previously for DNA oligonucleotides [7]. Under these conditions, some nanoparticles without PNA and some with more than one PNA molecule per nanoparticle can be expected to occur in addition to one nanoparticle/one PNA nanoconjugate species. The DNA oligonucleotides used to prepare target oligonucleotide dsDNA “dsr18” and PNA complementary molecular beacon “r18ASMB1” (with 6-carboxy-2',4',5',7',7'-hexachlorofluorescein as a fluorophore and dabcyI as a quencher) were obtained from Sigma Genosys. A noncomplementary dsDNA oligonucleotide “dsFM20” was prepared from “FM20” and “FM20AS” oligonucleotides. These oligonucleotides and a noncomplementary molecular beacon “MS5MB1” were also obtained from Sigma Genosys. All DNA oligonucleotides were kept as 100-mM stock solutions in TE buffer (10 mM Tris-HCl and 1 mM EDTA, pH 8) at -80 °C.

In some cases, either a short peptide segment of epidermal growth factor (pEGF) (N-term-RRRHIVRKRTLRR-C term) (Sigma-Genosys) containing a nuclear localization signal (NLS) or Alizarin Red S (Fluka) was conjugated to PNA-TiO₂ nanoconjugates to cover approximately 5% (9 molecules) or 10% (17 molecules) of the nanoparticle surface, respectively. The 3-nm TiO₂ nanoparticles have approximately 173 Ti atoms on the surface, each providing a potential binding site for one peptide or Alizarin Red S. Conjugation of these nanoparticle modifiers was confirmed by a shift in peak absorbance wavelength of the nanoconjugates compared with nanoparticles alone. In addition, Alizarin Red S is a fluorescent molecule (excitation 530–560 nm, emission 580 nm) and can be monitored using a fluoroi-mager (Typhoon Trio Variable Mode Imager).

Nanoparticles of colloidal TiO₂ were prepared as described in detail elsewhere [7]. The size of nanoparticles used in these experiments was 3 nm, rendering them avid in binding with dopamine-modified PNAs. At neutral pH (6–8), TiO₂ nanoparticles can be concentrated by centrifugal forces greater than 0.2 g.

The plasmid pKaede-MN1 (Marine Biological Laboratory) was used to investigate the ability of nanoconjugates to invade plasmid DNA. The oligonucleotides r18Sclone and r18ASclone (Table 1) formed a dsDNA insert that was cloned into *Eco*R1/*Xho*I sites of this plasmid, producing the recombinant pKaede-MN1-R18.

Gel electrophoresis

Hybridization reactions containing Alizarin Red S, ssDNA (67.0 μM), and either PNAs or PNA-TiO₂ nanoconjugates (33.5 μM) were heated to 95 °C for 2 min and cooled to room temperature over 3 h. Reactions were separated on 8–16% polyacrylamide gels (acrylamide/bisacrylamide 19:1, EMD Chemicals) in 1× TBE buffer (Sigma) for 2–3 h. Nanoparticles were visualized in wells of the gel, still contained within glass plates, by monitoring Alizarin Red S fluorescence by the Typhoon Trio Variable Mode Imager. DNA bands were visualized on the same gel after its removal from the glass plates and staining with GelStar (Cambrex). PNAs do not absorb this dye or several other DNA intercalating dyes [24]; therefore, they were visualized only in the context of hybrids with DNA.

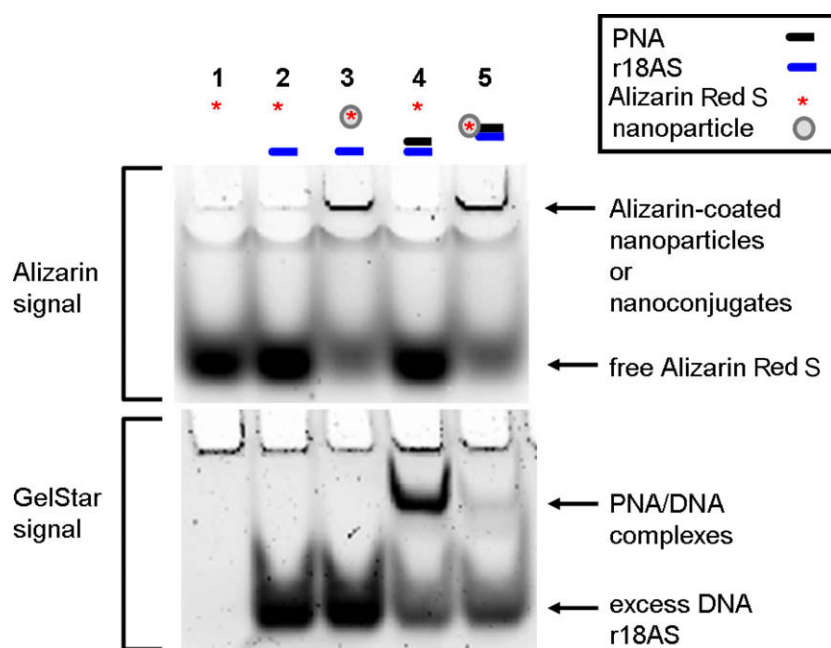


Fig. 1. PNA-TiO₂ nanoconjugates can be successfully conjugated and withstand incubation at 95 °C. Lanes 1–4 contain control reactions; lane 1 is free Alizarin Red S, lane 2 is a mixture of Alizarin Red S and complementary oligonucleotide DNA, lane 3 is Alizarin Red S-conjugated nanoparticle (without PNA) and complementary oligonucleotide DNA, and lane 4 contains a mixture of PNA (PNA-r18S), complementary oligonucleotide (r18AS), and Alizarin Red S. The test sample (lane 5) contains a mix of Alizarin Red S-coated TiO₂-PNA and twofold molar excess of complementary r18AS oligonucleotide DNA. All samples were heated to 95 °C for 2 min and cooled slowly to room temperature over 3 h to allow annealing. After cooling, samples were run on a 16% polyacrylamide gel for approximately 2 h and imaged for Alizarin Red S without separation of the gel from the glass plates that contained it. The same gel was taken out of the glass plates, stained with GelStar to visualize DNA and DNA/PNA hybrids, and then reimaged.

Nucleic acid hybridization monitoring using a real-time PCR apparatus

Hybridization reactions were monitored using a 7300 real-time PCR System (Applied Biosystems) and the following hybridization-dissociation protocol: 95 °C for 15 s, cooling to 4 °C, incubation at 4 °C for 30 s, and gradual reheating to 95 °C over approximately 1.25 h. HEX signal (for molecular beacons) or Power SYBR Green (Applied Biosystems) signal (for dsDNA) was recorded incrementally (~every 20 s) during the reheating phase. Hybridization and invasion reactions were also performed at 37–38 °C for 20 min, with HEX or Power SYBR Green signal being recorded incrementally throughout (~every 60 s). The average fluorescence measurement during this time was reported. All hybridization reactions involving molecular beacons (0.33 μM) contained nanoconjugates or free PNAs (0.66 μM) in the presence of 10 mM sodium phosphate buffer (NaH₂PO₄). Unless otherwise noted, experiments using Power SYBR Green contained nanoconjugates or PNAs (1.0 μM) and complementary dsDNA oligonucleotides (0.5 μM). Fluorescence intensity values were calculated by automated Applied Biosystems software, as were dissociation curves and derivative dissociation curves.

Plasmid invasion

Nanoparticles and nanoconjugates used in plasmid invasion studies were partially coated with Alizarin Red S (surface coverage was 10% or 17 molecules of Alizarin Red S per nanoparticle). Plasmid precipitation was done by taking advantage of the fact that in neutral pH buffers 3-nm TiO₂ nanoparticles can be concentrated by centrifugation at 0.2 g. Nanoparticles or nanoconjugates (115 nM) was mixed with supercoiled plasmid DNA (57.5 nM) in sodium phosphate buffer with 137 mM sodium and incubated for 2 h at 37 °C to allow for dsDNA invasion. Centrifugation for 10 min at 0.2 g followed; the pellet was washed by the same buffer and resuspended. Following a second wash, samples were loaded onto

a gel and subjected to electrophoresis. Due to the large size of the plasmid DNA, the force of electrophoresis separated plasmid molecules from nanoconjugates, allowing the plasmids to enter into the gel.

Statistical analyses

Statistical significance of differences were determined through analyses of variance (ANOVAs) followed by Tukey's honest significant difference multiple comparison tests using Systat 10.2 statistical analysis software (Systat Software). The bar graphs show means of three independent experiments with standard errors (SE) and statistical significance, with the latter indicated by an asterisk (*) as described in each figure legend.

Results

Conjugation of PNA-TiO₂ nanoconjugates and hybridization to complementary DNA

To demonstrate the conjugation efficiency of the PNA-TiO₂ nanoconjugates, we used to our advantage the fact that TiO₂ nanoparticles do not enter into polyacrylamide gels during typical electrophoresis [7]. To image the nanoparticles, we conjugated to them the fluorescent agent Alizarin Red S [5], whereas nucleic acids (ssDNA and ssDNA/PNA hybrids) were stained by GelStar dye after the electrophoresis. All nucleic acids used throughout this study are listed in Table 1. Hybridization reactions and controls were run on a polyacrylamide gel and imaged first for Alizarin Red S, and then they were stained with GelStar to visualize DNA. In lane 4 of Fig. 1, with a 1:2 molar ratio of PNA and complementary oligonucleotide, a PNA/DNA band can be visualized, whereas no such band is notable in lane 5, with a 1:2 ratio of PNA-TiO₂ and complementary oligonucleotide. The vast majority of PNA in that lane is conjugated to the nanoparticle and, therefore, is not free to enter

Table 1
Nucleic acid sequences used in this study

Sequence name	Sequence (beginning with N-term or 5' end)
PNA	TTCCTTGGATGTGGT
r18S oligonucleotide (homologous to PNA sequence)	TTCCTTGGATGTGGT
r18AS oligonucleotide (complementary to PNA sequence)	ACCACATCCAAGGAAA
FM20 oligonucleotide	TTGCTTGGTAGACCAGGCTG
FM20AS oligonucleotide	CAGCCTGGTCTACCAAGCAA
r18AS molecular beacon (homologous to r18AS, complementary to r18S and PNA)	[MHEx]CCCCACCAC ATCCAAGGAAAAG GGG[MDAB]
MS5 molecular beacon (noncomplementary beacon)	[MHEx]CCCCGAGAGAG AGAGAGAGA GAGAGGGG[MDAB]
Sense strand of r18S clone	TCGAGTTTCCTTGGATGTGGTG
Antisense strand of r18AS clone	AATTCACCACATCCAAGGAAAC

the gel. Hence, conjugated TiO₂-PNAs withstand incubation at 95 °C.

To investigate the ability of PNA-TiO₂ nanoconjugates to hybridize to complementary target DNA, we used molecular beacons containing either a complementary or noncomplementary DNA sequence in their loop (Fig. 2A). Changes in molecular beacon fluorescence, due to hybridization to the nanoconjugate, were monitored using a standard dsDNA dissociation protocol (Applied Biosystems); anticipated results are shown schematically in Fig. 2A. When the molecular beacon exists alone (Fig. 2A, top panel) or does not contain a complementary target to the nanoconjugate (Fig. 2A, bottom panel), the molecular beacon exists primarily in the closed position at temperatures below the melting temperature of the stem and low fluorescence values can be expected. In either of these cases, a sigmoid increase in fluorescence will occur when temperatures are raised above the melting temperature of the molecular beacon stem and the beacon transforms to the open position. Conversely, when the molecular beacon contains a complementary target, hybridization of the nanoconjugate will increase the presence of the open species of the molecular beacon and raise fluorescence values at lower temperatures (Fig. 2A, middle panel). The addition of free TiO₂ nanoparticles (Fig. 2B, blue curve) had little effect on the shape of the curve produced by molecular beacon alone (Fig. 2B, black curve). The addition of PNA-TiO₂ nanoconjugates complementary to the molecular beacon resulted in a more than sixfold increase at the initial fluorescence measurement at 14 °C (Fig. 2B, purple curve); as expected, this ratio is eventually lost at temperatures melting the molecular beacon stem. None of these alterations in fluorescence curves was observed when the same dissociation analyses were performed using a molecular beacon with a noncomplementary target DNA sequence in the molecular beacon loop (Fig. 2C). On the other hand, the presence of increasing concentrations of competitor-nonlabeled oligonucleotide complementary to PNA (with a sequence identical to the loop of the molecular beacon) sequesters PNA-TiO₂ nanoconjugates and reduces the observed changes in fluorescence due to hybridization between the molecular beacon and PNA-TiO₂ nanoconjugate (Fig. 2D).

The hybridization abilities of PNA-TiO₂ nanoconjugates were further characterized by determining their capability to engage in strand exchange with dsDNA. We developed a new method to differentiate between DNA/DNA and PNA/DNA complexes (Fig. 3) based on a knowledge that DNA intercalating dyes show little or no binding to PNA/DNA complexes [24]. Testing of the DNA-binding dye Power SYBR Green (Applied Biosystems) for monitoring DNA dissociation revealed that this DNA dye yields a fluorescent signal that is strong in the presence of dsDNA but greatly reduced in the presence of PNA/DNA complexes (Fig. 3A). We then tested the ability of PNA-TiO₂ nanoconjugates to outcompete a homologous ssDNA sequence for a complementary ssDNA target, as determined by a decrease in the derivative of fluorescence intensity

peak at the melting temperature of the DNA duplex. Samples containing oligonucleotide dsDNA yielded a characteristically sharp peak, indicative of the increased rate of fluorescence loss at the melting temperature (Fig. 3B, black curve). The addition of free glycidyl isopropyl ether-coated nanoparticles had little effect on the fluorescence curve, although a small increase in the peak was observed, perhaps due to nanoparticle concentration-induced stabilization of the duplex or background fluorescence from the nanoparticle (Fig. 3B, blue curve). However, the addition of PNA-TiO₂ nanoconjugates resulted in more than a 50% decrease in the fluorescence derivative peak at the melting temperature of the dsDNA, indicative of reduced dsDNA at this stage (Fig. 3B, purple curve). The addition of free PNAs to dsDNA oligonucleotides yielded similar results, affirming that PNA also competes during hybridization (Fig. 3B, red curve). The magnitude of this signal dampening effect was dependent on the quantity of PNA-TiO₂ nanoconjugates added (Fig. 3C), and such reductions in fluorescence and the rate of fluorescence loss were not obtained when PNA-TiO₂ nanoconjugates were added to samples of heterologous dsDNA oligonucleotides (Fig. 3D). This indicates that the changes in fluorescence were sequence specific and caused by the PNA-TiO₂ nanoconjugate outcompeting the homologous DNA strand for hybridization with the complementary DNA strand.

Modifications of the nanoparticle surface

PNA-TiO₂ nanoconjugates are capable of binding bidentate ligands enabling attachment of additional intracellular targeting agents and/or therapeutic payloads; moreover, carboxyl groups of peptides bind weakly to the nanoparticle surface. Therefore, it is essential to determine the effect of adding such a peptide on the ability of PNA-TiO₂ nanoconjugates to hybridize to target DNA. Hybridization-dissociation studies conducted with PNA-TiO₂ nanoconjugates coated with pEGF containing an NLS indicate that peptide-modified nanoconjugates maintain the ability to hybridize to complementary molecular beacons (Fig. 4A, purple curve). Peptide-coated nanoconjugates appear to have slightly enhanced hybridization capabilities compared with their naked counterparts (cf. fluorescence values at 14 °C in Fig. 2B, purple curve, and Fig. 4A, purple curve), perhaps due to a locally increased DNA concentration induced by the positively charged peptides. Such relative comparisons between figures were possible because all experimental conditions were set against the same intraexperimental molecular beacon controls. This suggests that peptide coating not only is a useful tool to increase cellular uptake (reviewed in Ref. [11]) but may also be improving interactions between the nanoconjugate and its molecular beacon target. Interestingly, when the PNA alone in the presence of pEGF peptide was used, the molecular beacon showed an aberrant fluorescence curve, perhaps due to interference between the free peptides and reopening of the molecular beacon (Fig. 4A, blue curve). Because no such inhibition was observed with

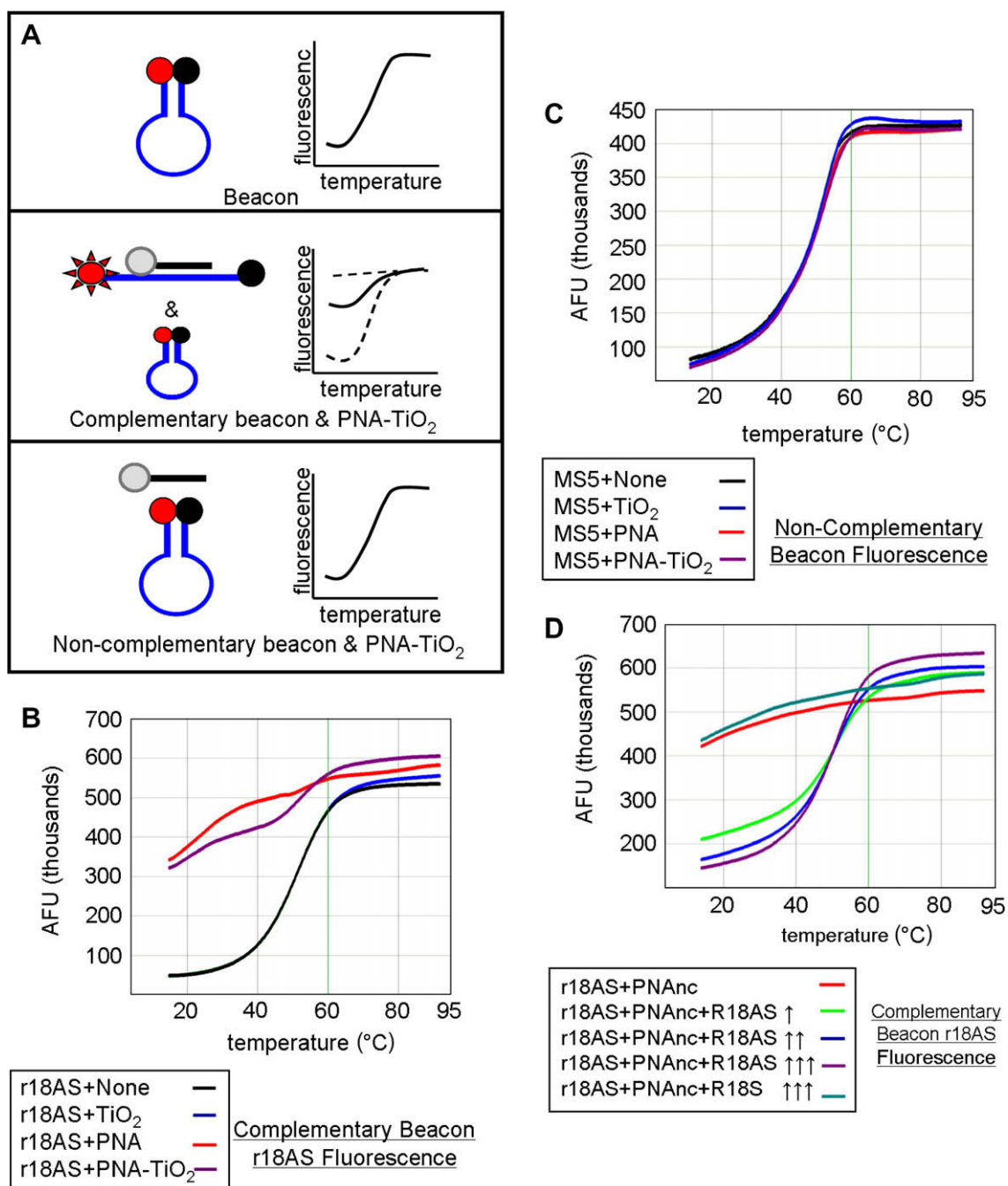


Fig. 2. TiO₂-PNA nanoconjugates can hybridize to complementary DNA. (A) Schematic representation depicts changes in fluorescence resulting from self-hybridization and melting of molecular beacons, changes in fluorescence caused by hybridization between molecular beacons and PNA-TiO₂ and self-hybridization and melting of molecular beacon, and changes in fluorescence when noncomplementary PNA-TiO₂ and molecular beacon are mixed. (B and C) Representative dissociation curves resulting from hybridization reactions containing test samples and complementary molecular beacon (B) or noncomplementary molecular beacon (C) are shown. Hybridization of either PNA-TiO₂ or PNA to molecular beacons containing a complementary target results in alterations in fluorescence curves, whereas no such alterations are observed when a noncomplementary molecular beacon is used. (D) The addition of various amounts of excess unlabeled PNA-complementary DNA oligonucleotide (r18AS), as molecular beacon competitor, to samples containing PNA-TiO₂ or PNA and complementary molecular beacons gradually returns the shape of the fluorescence curve to that obtained with samples containing molecular beacons alone. The addition of excess oligonucleotide identical to the sequence of PNA (r18S) shows a slight increase of the fluorescence (which can be expected because of additional hybridization of these DNA oligonucleotides with the beacon). In this and all other molecular beacon experiments, the concentration of PNA-TiO₂ and/or PNAs was 0.66 μM and the concentration of beacon was 0.33 μM. Concentrations of competitor in this experiment were as follows: ↑, 0.66 μM; ↑↑, 1.0 μM; ↑↑↑, 1.25 μM. AFU, arbitrary fluorescent units. The results shown are representative examples from five independent experiments.

the addition of peptide-coated nanoconjugates or nanoparticles (Fig. 4A, red curve), the ability of TiO₂ to readily bind surface modifiers and alter their function is further accentuated.

Previous studies have noted that Alizarin Red S bound to the surface of the nanoparticle permits visualization either in cells [11] or *in vitro* (Fig. 1). Hybridization-competition assays were

done to determine whether Alizarin Red S, when bound to the nanoparticle, affects hybridization of PNA bound to the same nanoparticle. Alizarin Red S-coated PNA-TiO₂ nanoconjugates demonstrated an ability to outcompete homologous DNA in binding with the complementary DNA target, as indicated by a sevenfold decrease in the fluorescence derivative peak (Fig. 4B, cf. blue and

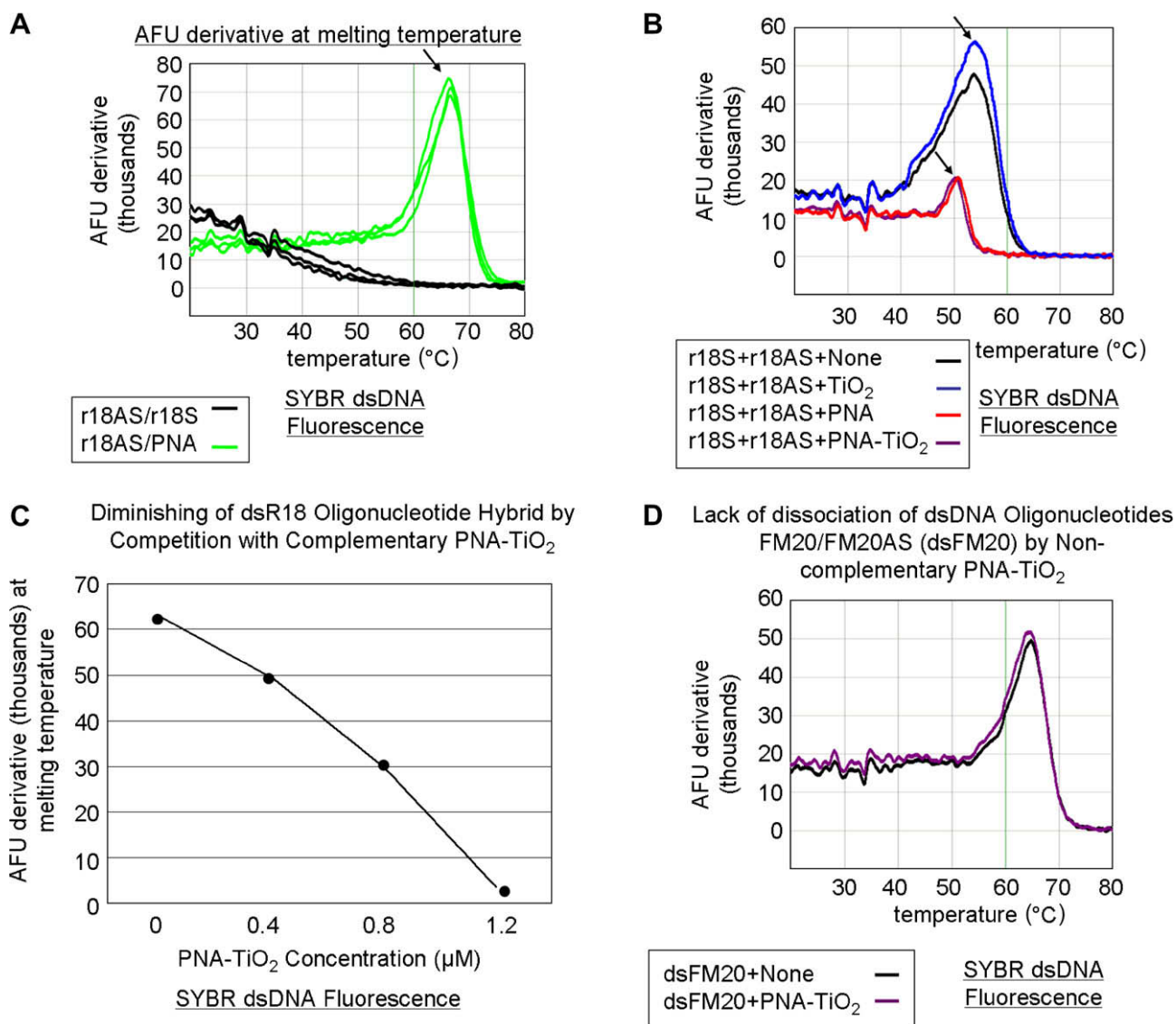


Fig. 3. PNA-TiO₂ nanoconjugates outcompete (replace) homologous DNA oligonucleotides in formation of the double-stranded hybrid (labeled R18 when made of two DNA oligonucleotides). (A) Derivative dissociation curves of fluorescence intensities show a well-defined melting temperature (T_m) peak (indicated by an arrow) for dsDNA hybrids (green) but not PNA/DNA complexes (black) (three replicates each). (B) Derivative dissociation curves show a lowering of the T_m peak height associated with competition between the homologous DNA strand of dsR18 and PNA or PNA-TiO₂ for the same target (complementary DNA oligonucleotide). Black arrows point to the AFU derivative at the T_m . (C) A graph showing inverse dependence of the peak height for the value of AFU derivative at the T_m peak related to the concentration of TiO₂-PNA nanoconjugates added to oligonucleotides creating dsR18 molecules is shown. (D) Representative derivative dissociation curves show no change in the T_m peak intensity when PNA-TiO₂ is combined with the noncomplementary dsDNA (hybrid of FM20 and FM20AS oligonucleotides, labeled dsFM20). In these and other experiments where Power SYBR Green signal was used for measurements, the concentration of complementary DNA oligonucleotides (r18S and r18AS) was 0.5 μM, whereas the nanoconjugate and PNA concentration was 1 μM. AFU, arbitrary fluorescence units.

purple curves). Therefore, Alizarin Red S coating did not adversely affect the hybridization behavior of nanoconjugates; in fact, coating the nanoconjugate enhanced the hybridization abilities by a factor of 2.5 compared with naked nanoconjugates and naked PNAs (cf. Figs. 4B and 3B). Furthermore, Alizarin Red S-coated PNA-TiO₂ nanoconjugates proved to be able to engage in strand exchange in 137-mM sodium buffer at 37 °C, as indicated by a reduction in Power SYBR Green fluorescence in reactions containing dsDNA and nanoconjugates compared with only dsDNA (Fig. 4C, $P < 0.05$).

Ability of PNA-TiO₂ nanoconjugates to invade plasmid DNA containing a mixed-base target under physiological-like temperature and ionic conditions

The use of PNA-TiO₂ nanoconjugates in cellular and whole animal systems depends on their ability to hybridize to complemen-

tary DNA under physiological-like conditions. Sodium concentration affects hybridization of DNA oligonucleotides [25] and PNA strand invasion of duplex DNA [26,27]. In addition, targeting of PNAs to previously inaccessible mixed-base sequences will allow increased diversification of potential therapeutic targets. Testing of PNA nanoconjugate behavior under physiological-like temperature and ionic conditions showed that PNA-TiO₂ nanoconjugates hybridized well with molecular beacons under such varied conditions (see Supplemental Fig. 1A and B in supplementary material). To affirm that PNA nanoconjugates are able to invade a supercoiled plasmid DNA containing a mixed-base target under physiological-like salt and temperature conditions (137 mM sodium and 37.5 °C), we conducted the experiments presented in Fig. 5. For these studies, we developed an assay based on the concentration of TiO₂ nanoparticles from aqueous solutions of neutral pH (whereas plasmid DNA does not concentrate in 100% aqueous

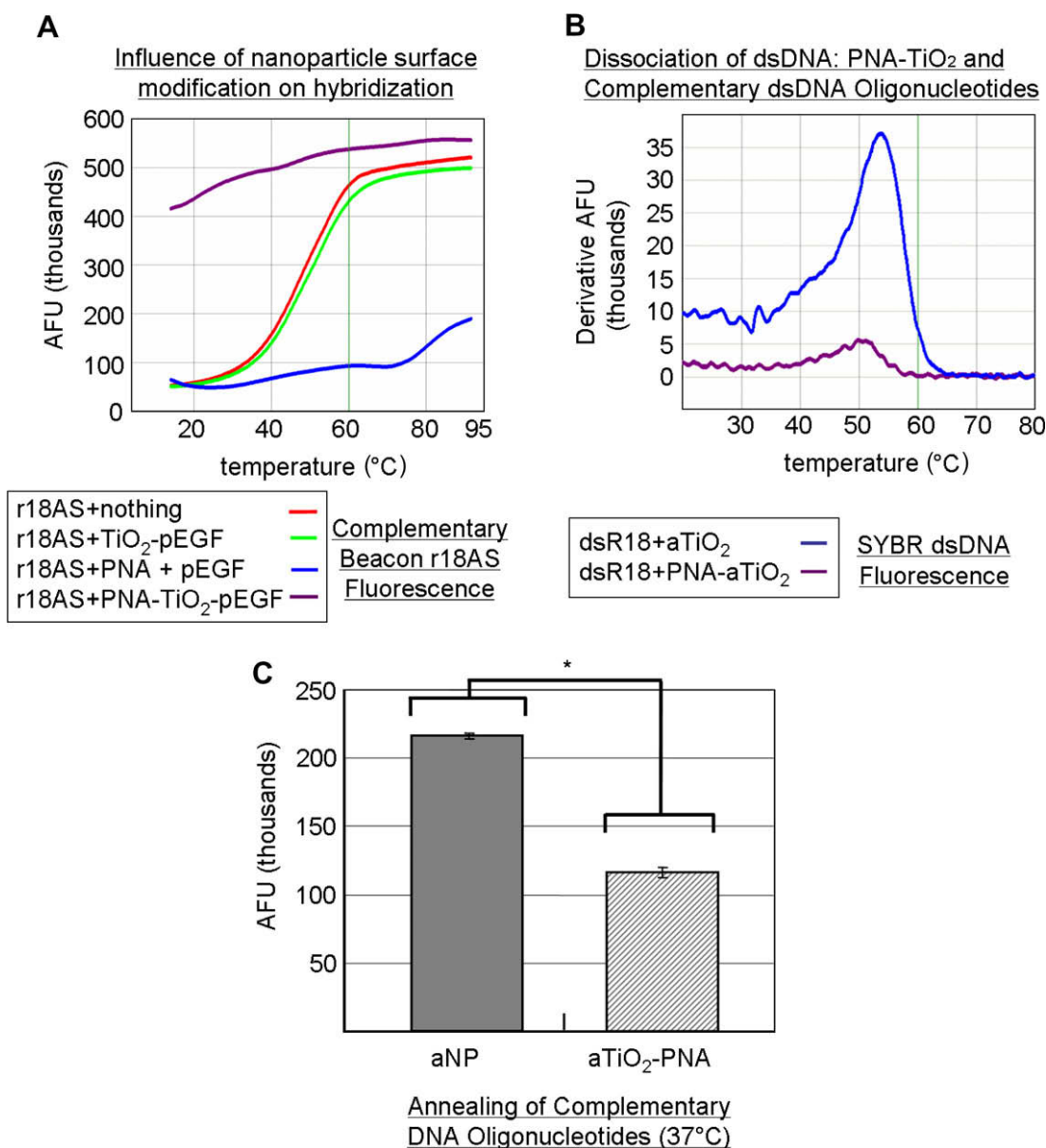


Fig. 4. PNA-TiO₂ nanoconjugates retain their hybridization abilities after additional modification of the nanoparticle. (A) PNA-TiO₂ nanoconjugates conjugated with pEGF maintain the ability to hybridize to target molecular beacon. Representative dissociation curves resulting from hybridization–dissociation reactions containing various test samples and a complementary molecular beacon are shown. Hybridization of either PNA-TiO₂ or PNA to molecular beacon r18AS results in alterations in fluorescence curves. (B) Alizarin Red S-coated PNA-TiO₂ nanoconjugates (PNA-aTiO₂) maintain the ability to outcompete homologous DNA oligonucleotide from an r18S/r18AS dsDNA hybrid (dsR18) oligonucleotide. Derivative dissociation curves show a lowering of the melting temperature (*T_m*) peak height associated with the addition of PNA-aTiO₂ to complementary DNA hybridization mixture. (C) PNA-aTiO₂ nanoconjugates are able to engage in strand exchange with dsDNA at 37 °C under 137-mM sodium conditions, while Alizarin Red S-coated TiO₂ nanoparticles (aNP) are not. AFU, arbitrary fluorescent units. *P* < 0.05.

solutions) when centrifuged at 0.2 g. pKaede-MN1 (MLB) and pKaede-MN1-R18 plasmids were used, and the only difference between these plasmids was that the latter contains a mixed-base sequence that is complementary to the sequence of PNA-TiO₂ nanoconjugate (depicted schematically in Fig. 5A). All reactions were incubated at 37.5 °C for 2 h with periodic mixing followed by centrifugations at 0.2 g to pellet nanoparticles or nanoconjugates. The presence of plasmid DNA in the pellet was then analyzed on an agarose gel (Fig. 5B). Three independent experiments are seen on this gel.

As expected, virtually no plasmid was recovered by centrifugation when the plasmid was incubated alone in the aqueous solution (Fig. 5B, lanes labeled 1). When Alizarin Red S-coated nanoparticles were incubated with the plasmid (Fig. 5B, lanes labeled 2)

or when Alizarin Red S-coated nanoconjugates were incubated with plasmid pKaede-MN1 devoid of a complementary insert R18 (Fig. 5B, lanes labeled 3), a small amount of plasmid was precipitated. However, a significant quantity of plasmid material was recovered when PNA-aTiO₂ nanoconjugates were incubated with the plasmid pKaede-MN1-R18 containing a complementary sequence R18 (Fig. 5B, lanes labeled 4). The limited precipitation of the plasmid found in samples 2 and 3 can be explained by non-sequence-specific interaction between the surface of nanoparticles and polyphosphate of the DNA backbone; the affinity of TiO₂ surface sites for polyphosphates was established previously in the literature [28]. Comparisons of these results indicate that recovery of the plasmid in reaction mixture containing TiO₂-PNA and supercoiled plasmid with the target sequence was due to the invasion

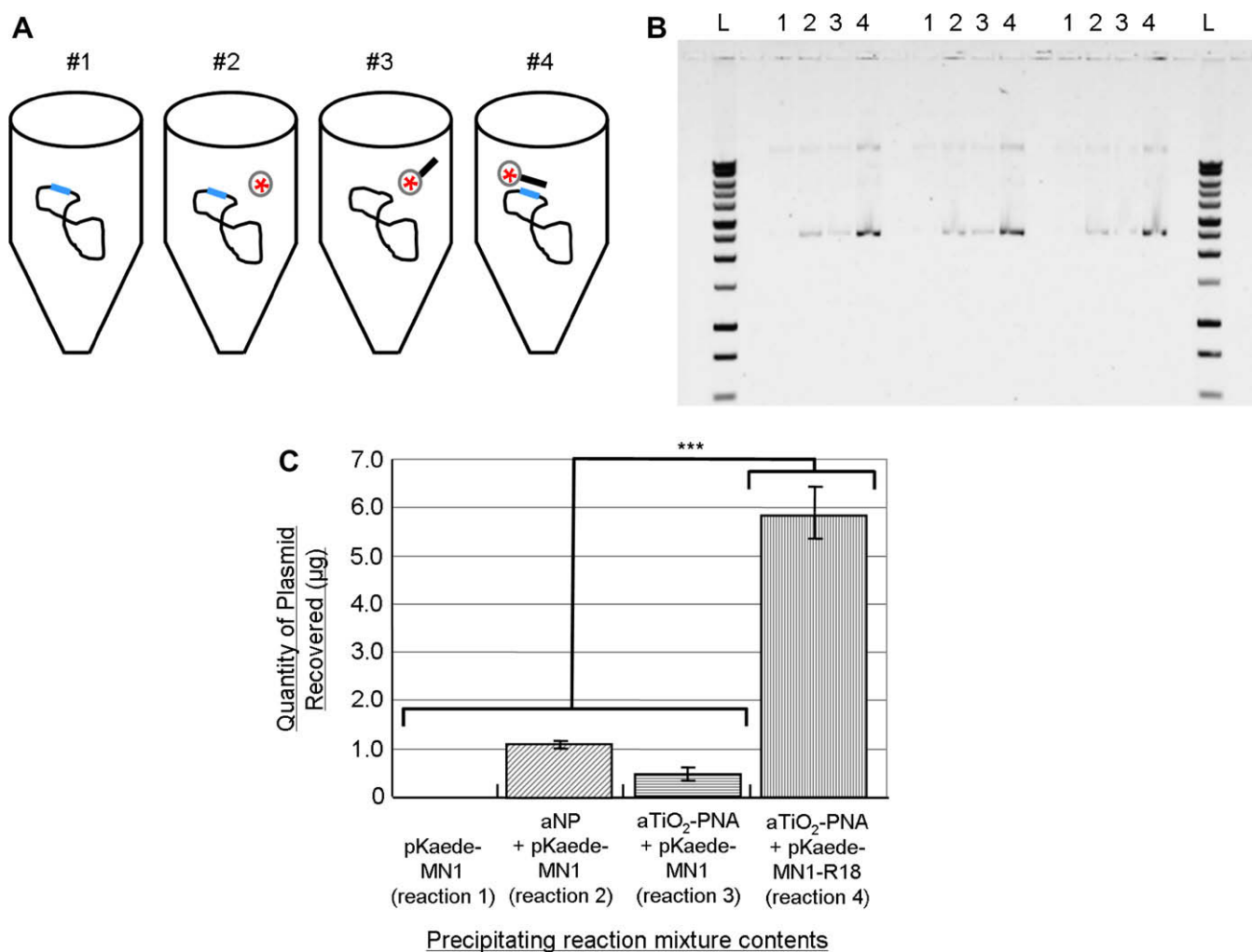


Fig. 5. (A) Schematic of the experimental design for sample preparation for each well type on the gel is shown. Reactions of types 1, 2, and 4 contained plasmid pKaede-MN1-R18 (containing the insert that is complementary to the PNA sequence); in addition, reaction type 2 contained Alizarin Red S-coated TiO₂ nanoparticles (aNP) and reaction type 4 also contained Alizarin Red S-coated PNA-TiO₂ nanoconjugates (aTiO₂-PNA). Reaction type 3 contained plasmid pKaede-MN1 without PNA target sequence and Alizarin Red S-coated PNA-TiO₂ nanoconjugates (aTiO₂-PNA). (B) Gel demonstrates the ability of PNA-TiO₂ nanoconjugates to invade target-containing plasmid DNA pKaede-MN1-R18 (wells containing reaction type 4), at 37 °C in 137 mM sodium, much more avidly than the “empty” pKaede-MN1 plasmid (wells containing reaction type 3), thereby allowing plasmid concentration by precipitation from a 100% aqueous solution. L, DNA ladder. In lanes 1–4, top bands are relaxed plasmids and bottom bands are supercoiled plasmids. Three separate experiments are shown on the same gel. (C) Semiquantitative comparison of plasmid precipitation resulting from reaction types 2–4 is shown. ... $P < 0.001$.

of the supercoiled plasmid DNA (reaction mixture 4) by nanoconjugates in a sequence-specific manner. The rate of plasmid recovery (Fig. 5C) suggests that 5.9 μg of the 19.5- μg plasmid sample (30% recovery rate) was achieved by precipitation of plasmid containing the mixed-base DNA target using TiO₂-PNA.

Discussion

Advances in nanoparticle technology have provided biologists with a set of new tools with unique physicochemical properties [4–6,11,29]. Previous research from our laboratory was focused on the properties of conjugates of DNA and TiO₂ nanoparticles, their synthesis, their use in enzymatic reactions (e.g., PCR), cleavage of DNA on excitation, and imaging by X-ray fluorescence microscopy [7,8]. Optically fluorescent agents that are ortho-substituted enediol ligands [5,6,11] may be added to the nanoconjugate to provide a new dimension to intracellular studies—imaging by confocal fluorescent microscopy [11]. As discussed previously, the nanoparticle can be further modified and detected with multiple other imaging modalities, including those that are of interest to medicine [9,10].

The main benefits of using TiO₂ nanoparticles are that they can serve as a platform/scaffold to which numerous molecules can be conjugated and, therefore, serve as a multimodal imaging agent and therapeutic agent; moreover, when excited by white light [7], these nanoconjugates have the ability to cleave DNA. The benefits of these nanoconjugates will, however, depend largely on their targeting and retention specificity, and these can be provided by conjugating DNA analogs to the nanoparticle surface in addition to any other targeting, diagnostic, and therapeutic modifications. Studies from our laboratory have shown that conjugating DNA to the nanoparticle surface greatly enhances cellular localization and retention of TiO₂ nanoparticles [7,8]. Replacing DNA with PNA will lead to increased stability of the nucleic acid component of the nanoconjugate and, therefore, will prolong the targeting life of the nanoconjugates and may even increase their sequence selectivity. Previously, fluorescently tagged homopyrimidine PNAs had been used to invade plasmid DNA for tracking without disturbing transgene expression [30]. However, to our knowledge, the current work is the first study demonstrating that modified, mixed-based PNAs are capable of invading and labeling supercoiled plasmid DNA. Development of PNA-TiO₂ nanoconjugates and their ability

to invade mixed-base sequences will undoubtedly enhance the targeting of deleterious cellular DNA in manners previously not possible. On the other hand, PNA/PNA binding affinity is extremely strong and often results in unwanted interactions. For this reason, it was essential to fully characterize PNA-TiO₂ nanoconjugates containing a low surface density of PNAs as in this study, before introducing additional variables in the form of potential PNA/PNA interactions.

To our knowledge, no previous studies have characterized factors affecting hybridization behaviors of PNAs conjugated to TiO₂ nanoparticles, so direct comparisons between the current results and others is not possible. In a different nanoparticle regime, PNAs conjugated to gold (Au) nanoparticles and immobilized on glass had the ability to discriminate between DNA targets with a single-base mismatch [31]. Numerous other studies involving Au nanoparticles have demonstrated single-base hybridization specificity of nucleic acid-nanoparticle conjugates by using various methods such as gel electrophoresis, DNA arrays combined with a traditional flatbed scanner, single-strand-specific nucleases, and high-fidelity DNA ligases [32–35]. In addition, DNA oligonucleotides conjugated to Au nanoparticles showed higher binding affinities and a more rapid melting transition compared with free oligonucleotides; this system was sensitive to many factors, including DNA surface density, nanoparticle size, salt concentration, and interparticle distances [36–38]. Using TiO₂ nanoparticles linked to ssDNA, it was demonstrated recently that a single-base mismatch between the nanoconjugate and its target significantly reduces photocatalytic cleavage due to disruption of the π stack, indicating that nucleic acid-TiO₂ nanoconjugates can also exhibit a high level of sequence specificity [39]. Under these circumstances, there is no reason to suspect that PNA-TiO₂ nanoconjugates would exhibit less sequence specificity. Relative differences in melting temperatures between Au-DNA nanoconjugates and free DNAs (compared with PNA-TiO₂ nanoconjugates and free PNAs) may be explained by many factors, including the increased nucleic acid surface density of Au-DNA nanoconjugates compared with PNA-TiO₂ nanoconjugates, as well as the dissimilar nucleic acid backbone. Au-DNA nanoconjugates are able to migrate through gels during electrophoresis [40], whereas DNA-TiO₂ [7] or PNA-TiO₂ nanoconjugates do not (Fig. 1); this suggests that Au and TiO₂ nanoparticles differentially affect the nucleic acids to which they are conjugated. Considering that Au is a noble metal, whereas TiO₂ is a semiconductor with very reactive surface chemistry, these differences should be expected. These studies highlight the complexity of hybridization dynamics involving nucleic acid-conjugated nanoparticles and emphasize the need for further studies of the effect of factors modulating hybridization between PNA-TiO₂ nanoconjugates and target DNA.

Conjugating peptides or imaging agents to the TiO₂ nanoparticles will aid in cellular uptake and visualization of PNA-TiO₂ nanoconjugates during intracellular studies. In addition, the imaging agent Alizarin Red S can be conjugated to TiO₂ nanoparticles and serve as a fluorescent marker. This study demonstrates that PNA-TiO₂ nanoconjugates coated with peptide segment of EGF or Alizarin Red S have an improved ability to hybridize to complementary DNA; these modifications will lead to enhanced cellular targeting and visualization of PNA-TiO₂ nanoconjugates in cells without sacrificing the hybridization proficiency of the nanoconjugates. Moreover, it is possible that the presence of peptides may improve hybridization performance of nanoconjugates, as shown by a comparison of Fig. 2B with Fig. 4A. Studies have demonstrated that such additional modifications of the nucleic acid-TiO₂ nanoconjugates with various ligands do not impede intracellular hybridization of nanoconjugates. DNA-TiO₂ nanoconjugates,

coated with bulky gadolinium contrast agent for detection with MRI, retained their intracellular hybridization specificity and retention [9,10].

Research investigating charge transfer in PNA/DNA complexes is limited, but one study has shown that a charge injected into the PNA strand can be transferred to guanine doublets on the complementary strand DNA via a hopping mechanism [41]. TiO₂ nanoparticles larger than 2 nm have been shown to be capable of creating electropositive holes [6]. Viewing this finding in light of our current study indicates that, like their DNA counterparts, PNA-TiO₂ nanoconjugates larger than 2 nm could be used to induce DNA cleavage when excited.

It is well established in the literature that PNAs have a longer half-life *in vivo* and intracellularly compared with DNAs [42]. However, the same body of research established that PNAs are not as soluble as DNAs and that some PNA sequences have proved to be difficult to synthesize in the past. The later issues have since been circumvented with the development of automated synthesis protocols [43], whereas challenges of solubility and delivery of PNAs into cells have been solved by new solubilization strategies. For example, PNAs can be annealed to a negatively charged DNA oligonucleotide and complexed with cationic lipids for intracellular delivery [44,45]. Alternative methods of intracellular delivery of PNAs include synthesis of a PNA with an NLS [46], electroporation [47,48], and possibly microinjection. The studies shown here, however, suggest that in the context of PNA-TiO₂ nanoconjugates, many different molecules can be attached to the nanoparticle part of the nanoconjugate (and in multiple copies) to increase cellular uptake of nanoparticle-conjugated PNAs.

Conclusion

This study has shown that PNA-TiO₂ nanoconjugates are capable of hybridizing with target DNA in a sequence-specific manner regardless of conjugation of peptides or imaging agents to the nanoparticle surface and invasion of supercoiled plasmid DNA containing a mixed-base target. PNA stability (established in the literature) should make PNA-TiO₂ nanoconjugates very useful in other intracellular and *in vivo* studies, improving targeting specificity and increasing sequence-specific intracellular retention. Also, the new methods for investigation of nanoparticle-nucleic acid conjugate hybridization parameters described in this article will facilitate the study of other DNA and DNA analog-nanoparticle systems. The evidence shown here indicates that PNA-TiO₂ nanoconjugates are a viable alternative to their DNA counterparts and warrant further in-depth study.

Acknowledgments

The authors acknowledge T. Chew, D. Dean, Y. Fukui, J. Maser, C. Cruz, A. Babbo, and D. Jakubczak for their scientific advice as well as G. Brown for her support. We also acknowledge the National Institutes of Health (CA107467, EB002100, P50 CA89018, and U54CA119341).

Appendix A. Supplementary data

Supplementary data associated with this article can be found, in the online version, at doi:10.1016/j.ab.2008.08.020.

References

- [1] P. Gonzalez-Alegre, Therapeutic RNA interference for neurodegenerative diseases: from promise to progress, *Pharmacol. Ther.* 114 (2007) 34–55.
- [2] F. Natt, siRNAs in drug discovery: target validation and beyond, *Curr. Opin. Mol. Ther.* 9 (2007) 242–247.

- [3] L. Scherer, J.J. Rossi, M.S. Weinberg, Progress and prospects: RNA-based therapies for treatment of HIV infection, *Gene Ther.* 14 (2007) 1057–1064.
- [4] M.C. Roco, T.A. Weber, M.P. Henkart, T.A. Kalil, R. Trew, J.S. Murday, P.G. Yoshida, M.P. Casassa, R.D. Shull, I.L. Thomas, National Nanotechnology Initiative: The Initiative and Its Implementation Plan, Office of Science and Technology, Washington, DC, 2007.
- [5] T. Rajh, L.X. Chen, K. Lukas, T. Liu, M.C. Thurnauer, D.M. Tiede, Surface restructuring of nanoparticles: an efficient route for ligand–metal oxide crosstalk, *J. Phys. Chem. B* 106 (2002) 10543–10552.
- [6] T. Rajh, O. Poluektov, A.A. Dubinski, G. Wiederrecht, M.C. Thurnauer, A.D. Trifunac, Spin polarization mechanisms in early stages of photoinduced charge separation in surface-modified TiO₂ nanoparticles, *Chem. Phys. Lett.* 344 (2001) 31–39.
- [7] T. Paunesku, T. Rajh, G. Wiederrecht, J. Maser, S. Vogt, N. Stojicevic, M. Protic, B. Lai, J. Oryhon, M. Thurnauer, G. Woloschak, Biology of TiO₂-oligonucleotide nanocomposites, *Nat. Mater.* 2 (2003) 343–346.
- [8] T. Paunesku, S. Vogt, B. Lai, J. Maser, N. Stojicevic, K.T. Thurn, C. Osipo, H. Liu, D. Legnini, Z. Wang, C. Lee, G.E. Woloschak, Intracellular distribution of TiO₂-DNA oligonucleotide nanoconjugates directed to nucleolus and mitochondria indicates sequence specificity, *Nano Lett.* 7 (2007) 596–601.
- [9] P.J. Endres, T. Paunesku, S. Vogt, T.J. Meade, G.E. Woloschak, DNA-TiO₂ nanoconjugates labeled with magnetic resonance contrast agents, *J. Am. Chem. Soc.* 129 (2007) 15760–15761.
- [10] T. Paunesku, T. Ke, R. Dharmakumar, N. Mascheri, A. Wu, B. Lai, S. Vogt, J. Maser, K. Thurn, B. Szolc-Kowalska, A. Larson, R.C. Bergan, R. Omary, D. Li, Z.R. Lu, G.E. Woloschak, Gadolinium-conjugated TiO₂-DNA oligonucleotide nanoconjugates show prolonged intracellular retention period and T1-weighted contrast enhancement in magnetic resonance images, *Nanomedicine* (2008). PMID: 18567541.
- [11] K.T. Thurn, E.M.B. Brown, A. Wu, S. Vogt, B. Lai, J. Maser, T. Paunesku, G.E. Woloschak, Nanoparticles for applications in cellular imaging, *Nanoscale Res. Lett.* (2007), doi:10.1007/s11671-007-9081-5.
- [12] P.E. Nielsen, M. Egholm, R.H. Berg, O. Buchardt, Sequence-selective recognition of DNA by strand displacement with a thymine-substituted polyamide, *Science* 254 (1991) 1497–1500.
- [13] J.E. Summerton, Morpholinos and PNAs compared, in: C.G. Jansen, M.J. During (Eds.), *Peptide Nucleic Acids, Morpholinos, and Related Antisense Biomolecules*, Springer, New York, 2006.
- [14] V.V. Demidov, V.N. Potaman, M.D. Frankkamenetskii, M. Egholm, O. Buchardt, S.H. Sonnichsen, P.E. Nielsen, Stability of peptide nucleic acids in human serum and cellular extracts, *Biochem. Pharmacol.* 48 (1994) 1310–1313.
- [15] S.E. Hamilton, M. Iyer, J.C. Norton, D.R. Corey, Specific and nonspecific inhibition of transcription by DNA, PNA, and phosphorothioate promoter analog duplexes, *Bioorg. Med. Chem. Lett.* 6 (1996) 2897–2900.
- [16] K. Kaihatsu, B.A. Janowski, D.R. Corey, Recognition of chromosomal DNA by PNAs, *Chem. Biol.* 11 (2004) 749–758.
- [17] S.C. Brown, S.A. Thomson, J.M. Veal, D.G. Davis, NMR solution structure of a peptide nucleic acid complexed with RNA, *Science* 265 (1994) 777–780.
- [18] M. Eriksson, P.E. Nielsen, Solution structure of a peptide nucleic acid-DNA duplex, *Nat. Struct. Biol.* 3 (1996) 410–413.
- [19] L. Betts, J.A. Josey, J.M. Veal, S.R. Jordan, A nucleic acid triple helix formed by a peptide nucleic acid-DNA complex, *Science* 270 (1995) 1838–1841.
- [20] H. Rasmussen, J.S. Kastrop, J.N. Nielsen, J.M. Nielsen, P.E. Nielsen, Crystal structure of a peptide nucleic acid (PNA) duplex at 1.7 Å resolution, *Nat. Struct. Biol.* 4 (1997) 98–101.
- [21] B. Armitage, T. Koch, H. Frydenlund, H. Orum, H.G. Batz, G.B. Schuster, Peptide nucleic acid-anthraquinone conjugates: strand invasion and photoinduced cleavage of duplex DNA, *Nucleic Acids Res.* 25 (1997) 4674–4678.
- [22] K. Kaihatsu, R.H. Shah, X. Zhao, D.R. Corey, Extending recognition by peptide nucleic acids (PNAs): binding to duplex DNA and inhibition of transcription by tail-clamp PNA-peptide conjugates, *Biochemistry (Mosc.)* 42 (2003) 13996–14003.
- [23] I.V. Smolina, V.V. Demidov, V.A. Soldatenkov, S.G. Chasovskikh, M.D. Frankkamenetskii, End invasion of peptide nucleic acids (PNAs) with mixed-base composition into linear DNA duplexes, *Nucleic Acids Res.* 33 (2005) e146.
- [24] P. Wittung, S.K. Kim, O. Buchardt, P. Nielsen, B. Norden, Interactions of DNA binding ligands with PNA-DNA hybrids, *Nucleic Acids Res.* 22 (1994) 5371–5377.
- [25] S. Salzberg, Z. Levi, M. Aboud, A. Goldberger, Isolation and characterization of DNA-DNA and DNA-RNA, *Biochemistry (Mosc.)* 16 (1977) 25–29.
- [26] P.E. Nielsen, M. Egholm, R.H. Berg, O. Buchardt, Sequence specific inhibition of DNA restriction enzyme cleavage by PNA, *Nucleic Acids Res.* 21 (1993) 197–200.
- [27] N.J. Peffer, J.C. Hanvey, J.E. Bisi, S.A. Thomson, C.F. Hassman, S.A. Noble, L.E. Babiss, Strand-invasion of duplex DNA by peptide nucleic acid oligomers, *Proc. Natl. Acad. Sci. USA* 90 (1993) 10648–10652.
- [28] A. Michelmore, W.Q. Gong, P. Jenkins, J. Ralston, The interaction of linear polyphosphates with titanium dioxide surfaces, *Phys. Chem. Chem. Phys.* 2 (2000) 2985–2992.
- [29] T. Rajh, J.M. Nedeljkovic, L.X. Chen, O. Poluektov, M.C. Thurnauer, Improving optical and charge separation properties of nanocrystalline TiO₂ by surface modification with vitamin C, *J. Phys. Chem. B* 103 (1999) 3515–3519.
- [30] E. Hillery, F.M. Munkonge, S. Xenariou, D.A. Dean, F.W. Alton, Nondisruptive, sequence-specific coupling of fluorochromes to plasmid DNA, *Anal. Biochem.* 352 (2006) 169–175.
- [31] T. Endo, K. Kerman, N. Nagatani, Y. Takamura, E. Tamiya, Label-free detection of peptide nucleic acid-DNA hybridization using localized surface plasmon resonance based optical biosensor, *Anal. Chem.* 77 (2005) 6976–6984.
- [32] W. Qin, L. Yung, Nanoparticle-based detection and quantification of DNA with single nucleotide polymorphism (SNP) discrimination selectivity, *Nucleic Acids Res.* 35 (2007) e111.
- [33] T. Taton, C. Mirkin, R. Letsinger, Scanometric DNA array detection with nanoparticle probes, *Science* 289 (2000) 1757–1760.
- [34] Y. Chen, C. Hsu, S. Hou, Detection of single-nucleotide polymorphisms using gold nanoparticles and single-strand-specific nucleases, *Anal. Biochem.* 375 (2008) 299–305.
- [35] J. Li, X. Chu, Y. Liu, J. Jiang, Z. He, Z. Zhang, G. Shen, R. Yu, A colorimetric method for point mutation detection using high-fidelity DNA ligase, *Nucleic Acids Res.* 33 (2005) e168.
- [36] Z. Li, R. Jin, C.A. Mirkin, R.L. Letsinger, Multiple thiol-anchored DNA-gold nanoparticle conjugates, *Nucleic Acids Res.* 30 (2002) 1558–1562.
- [37] R. Jin, G. Wu, Z. Li, C.A. Mirkin, G.C. Schatz, What controls the melting properties of DNA-linked gold nanoparticle assemblies?, *J. Am. Chem. Soc.* 125 (2003) 1643–1654.
- [38] A.K. Lytton-Jean, C.A. Mirkin, A thermodynamic investigation into the binding properties of DNA functionalized gold nanoparticle probes and molecular fluorophore probes, *J. Am. Chem. Soc.* 127 (2005) 12754–12755.
- [39] T. Tachikawa, Y. Asanoi, K. Kawai, S. Tojo, A. Sugimoto, M. Fujitsuka, T. Majima, Photocatalytic cleavage of single TiO₂/DNA nanoconjugates, *Chemistry* 14 (2008) 1492–1498.
- [40] A. Fu, C.M. Meehl, J. Cha, H. Chang, H. Yang, A.P. Alivisatos, Discrete nanostructures of quantum dots/Au with DNA, *J. Am. Chem. Soc.* 126 (2004) 10832–10833.
- [41] B. Armitage, D. Ly, T. Koch, H. Frydenlund, H. Orum, H.G. Batz, G.B. Schuster, Peptide nucleic acid-DNA duplexes: long range hole migration from an internally linked anthraquinone, *Proc. Natl. Acad. Sci. USA* 94 (1997) 12320–12325.
- [42] B.M. McMahon, D. Mays, J. Lipsky, J.A. Stewart, A. Fauq, E. Richelson, Pharmacokinetics and tissue distribution of a peptide nucleic acid after intravenous administration, *Antisense Nucleic Acid Drug Dev.* 12 (2002) 65–70.
- [43] L.D. Mayfield, D.R. Corey, Automated synthesis of peptide nucleic acids and peptide nucleic acid peptide conjugates, *Anal. Biochem.* 268 (1999) 401–404.
- [44] D.A. Braasch, D.R. Corey, Synthesis, analysis, purification, and intracellular delivery of peptide nucleic acids, *Methods* 23 (2001) 97–107.
- [45] B. Herbert, A.E. Pitts, S.I. Baker, S.E. Hamilton, W.E. Wright, J.W. Shay, D.R. Corey, Inhibition of human telomerase in immortal human cells leads to progressive telomere shortening and cell death, *Proc. Natl. Acad. Sci. USA* 96 (1999) 14276–14281.
- [46] K. Braun, P. Peschke, R. Pipkorn, S. Lampel, M. Wachsmuth, W. Waldeck, E. Friedrich, J. Debus, A biological transporter for the delivery of peptide nucleic acids (PNAs) to the nuclear compartment of living cells, *J. Mol. Biol.* 318 (2002) 237–243.
- [47] J.G. Karras, M.A. Maier, T. Lu, A. Watt, M. Manoharan, Peptide nucleic acids are potent modulators of endogenous pre-mRNA splicing of the murine interleukin-5 receptor- α chain, *Biochemistry (Mosc.)* 40 (2001) 7853–7859.
- [48] M.A. Shammass, C.G. Simmons, D.R. Corey, R.J. Shmookler-Reis, Telomerase inhibition by peptide nucleic acids reverses “immortality” of transformed human cells, *Oncogene* 18 (1999) 6191–6200.